Nonlinear Dyn (2009) 56: 243–253
DOI 10.1007/s11071-008-9396-5

ORIGINAL PAPER

Chaos control of a nonlinear oscillator with shape memory alloy using an optimal linear control: Part II: Nonideal energy source

V. Piccirillo · J.M. Balthazar · B.R. Pontes Jr. · J.L.P. Felix

Received: 11 January 2008 / Accepted: 9 July 2008 / Published online: 12 August 2008

Abstract In Part II of this two-part work, we apply an optimal linear control technique to suppress chaotic behavior in a SMA oscillator, driven by a DC motor with limited power supply (Nonideal sources). Nonideal sources of vibrations of structures are those whose characteristics are coupled to the motion of the structure. Thus, in this case, an additional equation of motion is written, related to the motor rotation. Special attention is focused into the resonance region, when the nonideal excitation frequency is near the natural frequency of the SMA oscillator. Numerical results are presented, which show the efficiency of the method in resonance region. The ideal case, when we do not consider the interaction between an energy source and structure was considered in Part I of this paper.

Keywords Nonideal system · Shape memory · Linear feedback control · Resonance region

V. Piccirillo · J.M. Balthazar (✉) · B.R. Pontes Jr.
Department of Engineering Mechanical, UNESP–São Paulo State University, CP 473, 17033-360, Bauru, SP, Brazil
e-mail: jmbaltha@rc.unesp.br

V. Piccirillo
e-mail: viniciuspiccirillo@yahoo.com.br

B.R. Pontes Jr.
e-mail: brpontes@feb.unesp.br

J.M. Balthazar · J.L.P. Felix
Department of Statistic, Applied Mathematical and Computation, UNESP–São Paulo State University, CP 178, 13500-230, Rio Claro, SP, Brazil

J.L.P. Felix
e-mail: jorgelpfelix@yahoo.com.br

1 Introduction

SMAs have been mainly applied in medical science, and in electrical, aerospace, and mechanical engineering. Concerning the dissipation effect, SMAs' high damping capacity may be exploited in adaptive passive control employed in bridges and civil structures subjected to earthquakes, for example [1–4]. Paper [5] gave a state-of-the-art of the development of passive control devices based on SMAs up to 1999. Other authors have investigated applications of SMA composites for vibration and structural acoustic control [6, 7].

On the other hand, systems excited by ideal sources are typically predictable near resonance, i.e., a frequency response curve for the system closely approximates the system behavior over the entire frequency domain. We note that as the driving frequency increases toward the natural frequency, there is a corresponding increase in the amplitude. Once resonance is reached, the driving frequency reduces the amplitude, but at no point in the frequency domain curve is discontinuous. In contrast, a system driven by a nonideal energy source may exhibit some peculiar deviations.

We know that jump phenomenon is a nonlinear effect that appears, when a portion of the right branch of the frequency response curve becomes unstable and typically occurs in systems driven by nonideal energy sources, or when the curve bends over and becomes multivalued. As the driving frequency approaches the natural frequency, the vibrating system can suddenly jump from one side of resonance to the other. That is, the system operating in a steady state cannot realize certain frequencies near resonance. The jump appears on the frequency response curve as a discontinuity which indicates a region where steady state conditions do not exist [8].

For nonideal systems, if we consider the region before resonance on a typical frequency response curve, we note that as the power supplied to the source increases, the RPM of the motor increases accordingly. However, this behavior does not continue indefinitely. That is, as closer the DC motor speed moves toward the resonant frequency, more power is required to increase the motor speed. More formally, a large change in the power supplied to the motor results in a small change in the frequency, but a large increase in the amplitude of the resulting vibrations. Thus, near resonance it appears that additional power supplied to the motor only increases the amplitude of the response while having little effect on the RPM of the motor.

We remarked that jump phenomena and the increase in power required by a source operating near resonance are manifestations of a nonideal energy source and are often referred as Sommerfeld effect [8, 9] (of getting stuck in resonance: the motor may not have enough power to reach higher regimes with low energy consumption as most of its energy is applied to move the structure and not to accelerate the shaft.), that is, the structural response provides a certain energy sink (one of the problems often faced by designers is how to drive a vibrating system through resonance and avoid the energy sink described by Sommerfeld).

The study of nonideal vibrating systems, that is, when the excitation is influenced by the response of the system, has been considered a major challenge in theoretical and practical engineering science research. We have founded several other control devices for nonideal systems which are well described in [9–14].

In this paper, we investigated the linear control method based on the linear feedback control that has been reformulated under optimal control theory viewpoint and treated in more detail in [15–18]. The numerical implementation of this method demonstrated the effectiveness to control the chaotic motion in nonideal system. *This is a first use of this kind of control on nonideal vibrating system.*

2 Problem formulation

To describe the behavior of the SMAs' system, we will adopt a constitutive model described in Part I which consider, by definition (Apud [19]), the temperature and strain relation given by

$$\sigma = q(T - T_M)\varepsilon - b\varepsilon^3 + \frac{b^2}{4q(T_A - T_M)}\varepsilon^5,$$
$$T_A = T_M + \frac{b^2}{4qe} \tag{1}$$

where q and b are positive constants of the material, while T_A correspond to the temperature where the austenitic phase is stable, T_M corresponds to the temperature where the martensitic phase is stable and the constant e, may be expressed in terms of other constants of the material.

The adopted model of the vibrating system and the source of disturbance with a limited power supply are illustrated in Fig. 1. It consists of a mass M, a SMA element, and a linear damping with viscous damping coefficient c. On the object with mass M, a nonideal DC motor is placed, with a driving rotor of a moment of inertia J and r is the eccentrically of the considered unbalanced mass m.

In general, the mathematical modeling of this kind of problem (treated here) is represented by the following governing equations of motion [20]:

$$m_1\ddot{x} + f_1(x, \dot{x}) + f_2(x) = F(\dot{\phi}, \ddot{\phi}, \lambda),$$
$$J\ddot{\phi} + H(\dot{\phi}) = L(\dot{\phi}) + R(\phi, \dot{\phi}, \ddot{x}, \eta) \tag{2}$$

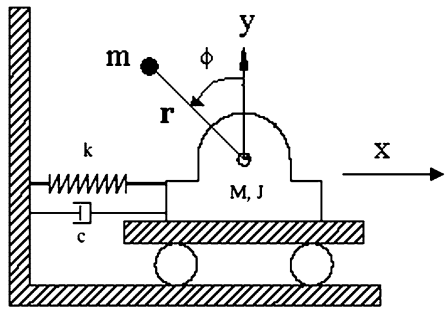

Fig. 1 Nonideal model with shape memory

where: $m_1 = m + M$, x is the displacement of SMA oscillator, ϕ is the angular displacement of the rotor, $F(\dot{\phi}, \ddot{\phi}, \lambda)$ express the action of the source of energy on the oscillating system (angular velocity of motor is not constant), λ and η are unbalanced coefficient, J is the moment of inertia of mass, the function $R(\phi, \dot{\phi}, \ddot{x}, \eta)$ express the action of the oscillating system on the source of energy, the function $H(\dot{\phi})$ is the resistive torque applied to the motor, the function $L(\dot{\phi})$ is the driving torque of the source of energy (motor), $f_1(x, \dot{x})$ is a damping term not necessary linear and $f_2(x)$ represent the SMA spring terms.

Note that usually the inductance is much smaller than the mechanical time constant of the system and then in stationary regime, we can take $L(\dot{\phi})$ as linear with $L(\dot{\phi}) = \xi_1 - \xi_2\dot{\phi}$, where ξ_1 is related to voltage applied across the armature of the DC motor, that is, a possible control parameter of the problem and ξ_2 is a constant for each model of DC motor considered.

Trough of the Lagrange's formulation, we obtain the following equation of motion [21]

$$\begin{cases} (M+m)\ddot{x} + c\dot{x} - mr\left(\ddot{\phi}\cos\phi - \dot{\phi}^2\sin\phi\right) \\ \quad + \bar{q}(T - T_M)x - \bar{b}x^3 + \bar{e}x^5 = 0, \\ \left(J + mr^2\right)\ddot{\phi} - mr\ddot{x}\cos\phi = \Gamma(\dot{\phi}). \end{cases} \tag{3}$$

Thus, the governing equations of motion of the system have the dimensionless form

$$\begin{cases} \ddot{u} + 2\mu\dot{u} + (\theta - 1)u - \alpha u^3 + \gamma u^5 \\ \quad - \lambda\left[\ddot{\phi}\cos\phi - \dot{\phi}^2\sin\phi\right] = 0, \\ \ddot{\phi} - \eta\ddot{u}\cos\phi = \xi_1 - \xi_2\dot{\phi} \end{cases} \tag{4}$$

where the dot represents dimensionless time differentiation and the variables are given by

$$\begin{aligned} u &= \frac{x}{L}, \qquad \tau = \omega_0 t, \qquad \omega_0^2 = \frac{qA_rT_M}{(M+m)L}, \\ \alpha &= \frac{bA_r}{(M+m)L\omega_0^2}, \qquad \theta = \frac{T}{T_M}, \\ \mu &= \frac{c}{2(M+m)\omega_0}, \qquad \gamma = \frac{eA_r}{(M+m)L\omega_0^2}, \\ \lambda &= \frac{mr}{(M+m)L}, \qquad \eta = \frac{mrL}{(J+mr^2)}. \end{aligned} \tag{5}$$

3 Optimal control design problem for SMA nonideal model

We apply the control method, following the ideas of the works [16, 17] to the SMA oscillator driven by a DC motor with limited power supply. We remarked that in present paper, using the above formulated theorem in order to determine the linear feedback control, we solve more general case of the control design problem for the nonideal system when a desired trajectory is a periodic orbit.

Equation (4) may be rewritten in the state variables form, as following

$$\begin{cases} \dot{u}_1 = u_2, \\ \dot{u}_2 = \frac{1}{1-\lambda\eta\cos^2 u_3}[\lambda((\xi_1 - \xi_2 u_4)\cos u_3 - u_4^2\sin u_3) + \alpha u_1^3 - \gamma u_1^5 - (\theta - 1)u_1 - 2\mu u_2], \\ \dot{u}_3 = u_4, \\ \dot{u}_4 = \frac{\xi_1}{1-\lambda\eta\cos^2 u_3} + \frac{\eta\cos u_3}{1-\lambda\eta\cos^2 u_3}[\alpha u_1^3 - \gamma u_1^5 - (\theta - 1)u_1 - 2\mu u_2 - \frac{\xi_2 u_4}{\eta\cos u_3} - \lambda u_4^2\sin u_3]. \end{cases} \tag{6}$$

The nonideal system, with the low control $Z(t)$ is described as

$$\begin{bmatrix} \dot{u}_1 \\ \dot{u}_2 \\ \dot{u}_3 \\ \dot{u}_4 \end{bmatrix} = \begin{bmatrix} u_2 \\ \frac{1}{1-\lambda\eta\cos^2 u_3}[\lambda((\xi_1 - \xi_2 u_4)\cos u_3 - u_4^2\sin u_3) + \alpha u_1^3 - \gamma u_1^5 - (\theta - 1)u_1 - 2\mu u_2] \\ u_4 \\ \frac{\xi_1}{1-\lambda\eta\cos^2 u_3} + \frac{\eta\cos u_3}{1-\lambda\eta\cos^2 u_3}[\alpha u_1^3 - \gamma u_1^5 - (\theta - 1)u_1 - 2\mu u_2 - \frac{\xi_2 u_4}{\eta\cos u_3} - \lambda u_4^2\sin u_3] \end{bmatrix} + BZ \tag{7}$$

where $B \in R^{n\times m}$ is a constant matrix $Z \in R^m$ is a control vector $m \leq 4$, $n = 4$.

Let the desired trajectory be a vector $\tilde{u} = [\tilde{u}_1(t)\ \tilde{u}_2(t)\ \tilde{u}_3(t)\ \tilde{u}_4(t)]^T$, which satisfies the following equation:

$$\begin{bmatrix} \dot{\tilde{u}}_1 \\ \dot{\tilde{u}}_2 \\ \dot{\tilde{u}}_3 \\ \dot{\tilde{u}}_4 \end{bmatrix} = \begin{bmatrix} \tilde{u}_2 \\ \frac{1}{1-\lambda\eta\cos^2\tilde{u}_3}[\lambda((\xi_1 - \xi_2\tilde{u}_4)\cos\tilde{u}_3 - \tilde{u}_4^2\sin\tilde{u}_3) + \alpha\tilde{u}_1^3 - \gamma\tilde{u}_1^5 - (\theta-1)\tilde{u}_1 - 2\mu\tilde{u}_2] \\ \tilde{u}_4 \\ \frac{\xi_1}{1-\lambda\eta\cos^2\tilde{u}_3} + \frac{\eta\cos\tilde{u}_3}{1-\lambda\eta\cos^2\tilde{u}_3}[\alpha\tilde{u}_1^3 - \gamma\tilde{u}_1^5 - (\theta-1)\tilde{u}_1 - 2\mu\tilde{u}_2 - \frac{\xi_2\tilde{u}_4}{\eta\cos\tilde{u}_3} - \lambda\tilde{u}_4^2\sin\tilde{u}_3] \end{bmatrix} + B\tilde{z} \tag{8}$$

where $\tilde{z}$ is a control vector which maintains the nonideal system in the desired trajectory.

Subtracting (8) from (7), the nonideal system may be expressed as

$$\dot{y} = Hy + g(y)y + Bz \tag{9}$$

where

$$H = \begin{bmatrix} 2 & 0 & 1 & 0 \\ 1 & 0 & 1 & 1 \\ 1 & 1 & 3 & 0 \\ 1 & 0 & 2 & 0 \end{bmatrix}, \qquad y = \begin{bmatrix} u_1 - \tilde{u}_1 \\ u_2 - \tilde{u}_2 \\ u_3 - \tilde{u}_3 \\ u_4 - \tilde{u}_4 \end{bmatrix}, \qquad z = \begin{bmatrix} Z_1 - \tilde{z}_1 \\ Z_2 - \tilde{z}_2 \\ Z_3 - \tilde{z}_3 \\ Z_4 - \tilde{z}_4 \end{bmatrix},$$

$$g(y) = \frac{1}{1-\lambda\eta\cos^2(y_3+\tilde{u}_3)}$$

$$\times \begin{bmatrix} -2y_1(1-\lambda\eta\cos^2(y_3+\tilde{u}_3)) & y_2(1-\lambda\eta\cos^2(y_3+\tilde{u}_3)) & y_3(1-\lambda\eta\cos^2(y_3+\tilde{u}_3)) & 0 \\ \begin{array}{l}[\lambda((\xi_1 - \xi_2(y_4+\tilde{u}_4))\cos(y_3+\tilde{u}_3) \\ \quad -(y_4+\tilde{u}_4)^2\sin(y_3+\tilde{u}_3)) \\ \quad +\alpha(y_1+\tilde{u}_1)^3 - \gamma(y_1+\tilde{u}_1)^5 \\ \quad -(\theta-1)(y_1+\tilde{u}_1) - 2\mu(y_2+\tilde{u}_2)] \\ \quad -\frac{1-\lambda\eta\cos^2(y_3+\tilde{u}_3)}{1-\lambda\eta\cos^2\tilde{u}_3}[\lambda((\xi_1 - \xi_2\tilde{u}_4) \\ \quad \times\cos\tilde{u}_3 - \tilde{u}_4^2\sin\tilde{u}_3) \\ \quad +\alpha\tilde{u}_1^3 - \gamma\tilde{u}_1^5 - (\theta-1)\tilde{u}_1 - 2\mu\tilde{u}_2] \\ \quad -y_1(1-\lambda\eta\cos^2(y_3+\tilde{u}_3)) \end{array} & 0 & -y_3(1-\lambda\eta\cos^2(y_3+\tilde{u}_3)) & -y_4(1-\lambda\eta\cos^2(y_3+\tilde{u}_3)) \\ y_1(1-\lambda\eta\cos^2(y_3+\tilde{u}_3)) & y_2(1-\lambda\eta\cos^2(y_3+\tilde{u}_3)) & -3y_3(1-\lambda\eta\cos^2(y_3+\tilde{u}_3)) & y_4(1-\lambda\eta\cos^2(y_3+\tilde{u}_3)) \\ \begin{array}{l}\xi_1 + \eta\cos(y_3+\tilde{u}_3)[\alpha(y_1+\tilde{u}_1)^3 \\ \quad -\gamma(y_1+\tilde{u}_1)^5 - (\theta-1)(y_1+\tilde{u}_1) \\ \quad -2\mu(y_2+\tilde{u}_2) - 2\mu(y_2+\tilde{u}_2) \\ \quad -\frac{\xi_2(y_4+\tilde{u}_4)}{\eta\cos(y_3+\tilde{u}_3)} - \frac{\xi_2(y_4+\tilde{u}_4)}{\eta\cos(y_3+\tilde{u}_3)} \\ \quad -\lambda(y_4+\tilde{u}_4)^2\sin(y_3+\tilde{u}_3)] \\ \quad -\frac{\xi_1(1-\lambda\eta\cos^2(y_3+\tilde{u}_3))}{1-\lambda\eta\cos^2\tilde{u}_3} \\ \quad +\frac{\eta\cos\tilde{u}_3(1-\lambda\eta\cos^2(y_3+\tilde{u}_3))}{1-\lambda\eta\cos^2\tilde{u}_3}[\alpha\tilde{u}_1^3 - \gamma\tilde{u}_1^5 \\ \quad -(\theta-1)\tilde{u}_1 - 2\mu\tilde{u}_2 \\ \quad -\frac{\xi_2\tilde{u}_4}{\eta\cos\tilde{u}_3} - \lambda\tilde{u}_4^2\sin\tilde{u}_3] \end{array} & 0 & -2y_3(1-\lambda\eta\cos^2(y_3+\tilde{u}_3)) & 0 \end{bmatrix}$$

where $y \in R^n$ is a state vector, $H \in R^{n\times n}$ is a bounded matrix, $B \in R^{n\times m}$ is a constant matrix, $z \in R^m$ is a control vector, and $g(y) \in R^n$ is a matrix, which elements are continuous nonlinear functions, $g(0) = 0$.

Table 1 Material constants for a Cu-Zn-Al-Ni alloy

q (MPa/K)	b (MPa)	e (MPa)	T_M (K)	T_A (K)
523.29	1.868×10^7	2.186×10^9	288	364.3

We remark that the choice of H is not unique, and this influences the performance of the resultant controller.

We know that in several problems of physics and engineering science, the chaotic regime is not desirable and the goal here is to find a control law z that leads the perturbed system to a desired one. These kinds of regimes may be an equilibrium point or a periodic or nonperiodic orbit. The vector y of the system (9), can be considered as the deviation of the perturbed trajectory of system from the desired one. In Part I of this work, we present an important result, concerning a control law that guarantees stability for a nonlinear system and minimizes a nonquadratic performance functional.

4 Numerical results

In this section, numerical simulations are carried out, in order to verify the effectiveness of above proposed method. In all numerical simulations, to analyze the behavior of the nonideal dynamical system, the spring is assumed to be made of a (Cu-Zn-Al-Ni) alloy with the properties presented in Table 1.

Furthermore, in all numerical simulations, we considered the parameters: $\mu = 0.01$, $\eta = 0.6$, $\lambda = 0.4$ and $\xi_2 = 1.5$. Note that the passage through the resonance is itself obtained, by varying the angular velocity $\dot{\phi}$ of the DC motor.

In order to illustrate, the response of the nonideal system, we consider a temperature where the martensitic phase is stable ($\theta = 0.7$). In a second situation, we analyze the response at higher temperatures ($\theta = 2$) when the alloy is fully austenitic. We also plotted the Poincare section which represents the surface of section $(u_1(\tau_n), u_2(\tau_n))$. The points $(u_1(\tau_n), u_2(\tau_n))$ are captured for $\tau_n = nT$, where $n = 1, 2, 3, \ldots$, with period $T = \frac{2\pi}{\Omega_M}$ [22]. The averaging angular velocity Ω_M is obtained numerically.

$$\Omega_M = \frac{\phi(\tau_1) - \phi(0)}{\tau_1} = \frac{u_3(\tau_1) - u_3(0)}{\tau_1} \tag{10}$$

where τ_1 is a long time period for numerical calculation.

The greatest interaction between the vibrating system and the energy source will occur at resonance. We define the resonance region as:

$$\frac{d\phi}{dt} - \omega_0 = O(\varepsilon) \tag{11}$$

where $\frac{d\phi}{dt}$ is the angular velocity, ε is the small parameter of the problem of the order of 10^{-3}. ω_0: natural frequency of the system.

Generally, for a wide range of physical parameters when the system was started from rest, the angular velocity of the rotor would increase until it reached the neighborhood of the natural frequency ω_0. Then depending upon physical parameters values $\frac{d\phi}{dt}$ would increase beyond the resonance region (*Pass Through*) or it remains close to ω_0 (*Capture*).

Next, we determined a first-order solution of (4) using the method of averaging [8], therefore, the desired periodic trajectory is considered as follows:

$$\begin{cases} \tilde{u}_1 = a\cos(\dot{\phi}_M t + \beta), \\ \tilde{u}_2 = \dot{\tilde{u}}_1, \\ \tilde{u}_3 = \dot{\phi}_M t, \\ \tilde{u}_4 = \dot{\tilde{u}}_3, \end{cases} \tag{12}$$

where a, β, and $\dot{\phi}_M$ are amplitude, phase, and average motor frequency, respectively.

Using the proposed feedback control design procedure, the chaotic motion of the nonideal system is tracked to the desired periodic orbit (12). Therefore, choosing

$$Q = \begin{bmatrix} 1 & 0 & 0 & 0 \\ 0 & 1 & 0 & 0 \\ 0 & 0 & 1 & 0 \\ 0 & 0 & 0 & 1 \end{bmatrix} \quad \text{and} \quad R = \begin{bmatrix} 1 & 0 & 0 & 0 \\ 0 & 1 & 0 & 0 \\ 0 & 0 & 1 & 0 \\ 0 & 0 & 0 & 1 \end{bmatrix}$$

we obtain

$$P = \begin{bmatrix} 4.3598 & 0.4660 & 2.2468 & 0.2245 \\ 0.4660 & 1.1550 & 1.6008 & 0.2962 \\ 2.2428 & 1.6008 & 6.5190 & 0.6921 \\ 0.2245 & 0.2962 & 0.6921 & 0.9876 \end{bmatrix} \tag{13}$$

and by solving the Riccati equation using the LQR function of MATLAB™, we obtain the linear feed-

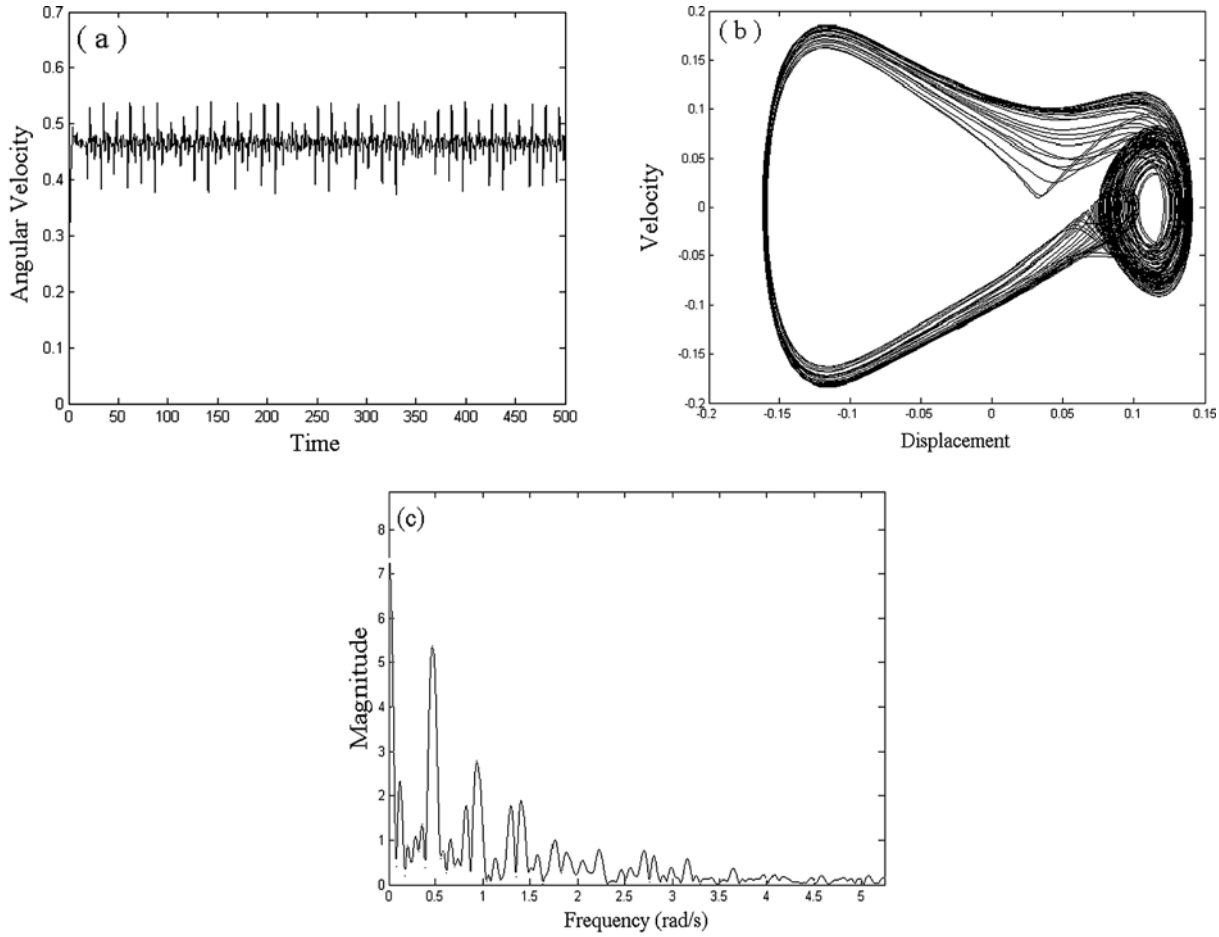

Fig. 2 Uncontrolled system: (**a**) Angular velocity time response, (**b**) Phase portrait, and (**c**) Power spectrum for the $\theta = 0.7$, $\mu = 0.01$, and $\xi_1 = 0.7$

back control below, and we reminisced that this control is optimal.

$$z = -\begin{bmatrix} 4.3598 & 0.4660 & 2.2468 & 0.2245 \\ 0.4660 & 1.1550 & 1.6008 & 0.2962 \\ 2.2428 & 1.6008 & 6.5190 & 0.6921 \\ 0.2245 & 0.2962 & 0.6921 & 0.9876 \end{bmatrix} y. \quad (14)$$

4.1 Martensitic phase

In this section, we are going to exhibit a series of numerical simulation to verify the performance of the linear feedback control for the nonideal system. In order to illustrate the response of the nonideal system, we assumed that the SMA spring is initially at a low temperature $\theta = 0.7$, and is in its martensite state. The parameters are selected as $\theta = 0.7$, $\mu = 0.01$, and $\xi_1 = 0.7$, thus we obtained that the system (4) without control possesses a chaotic attractor, shown in Fig. 2.

The control law of relations (14) with desired control is applied to the nonideal chaotic system in order to stabilize the unstable chaotic orbit of the system. Through of the averaging method, we cannot obtain the desired periodic orbit of (4) for $\theta = 0.7$. With this respect, (4), only can be determined for $\theta \geq 1$. Thus, the parameter considered for the desired periodic orbit is $\theta = 1.5$, $\mu = 0.01$ and $\xi_1 = 1.05$ (value in resonance region). In the stead-state phase, (12) has the following form:

$$\tilde{u} = \begin{bmatrix} 0.1357\cos(0.6999t + 4.703) \\ -0.095\sin(0.6999t + 4.703) \\ 0.6999t \\ 0.6999 \end{bmatrix}. \quad (15)$$

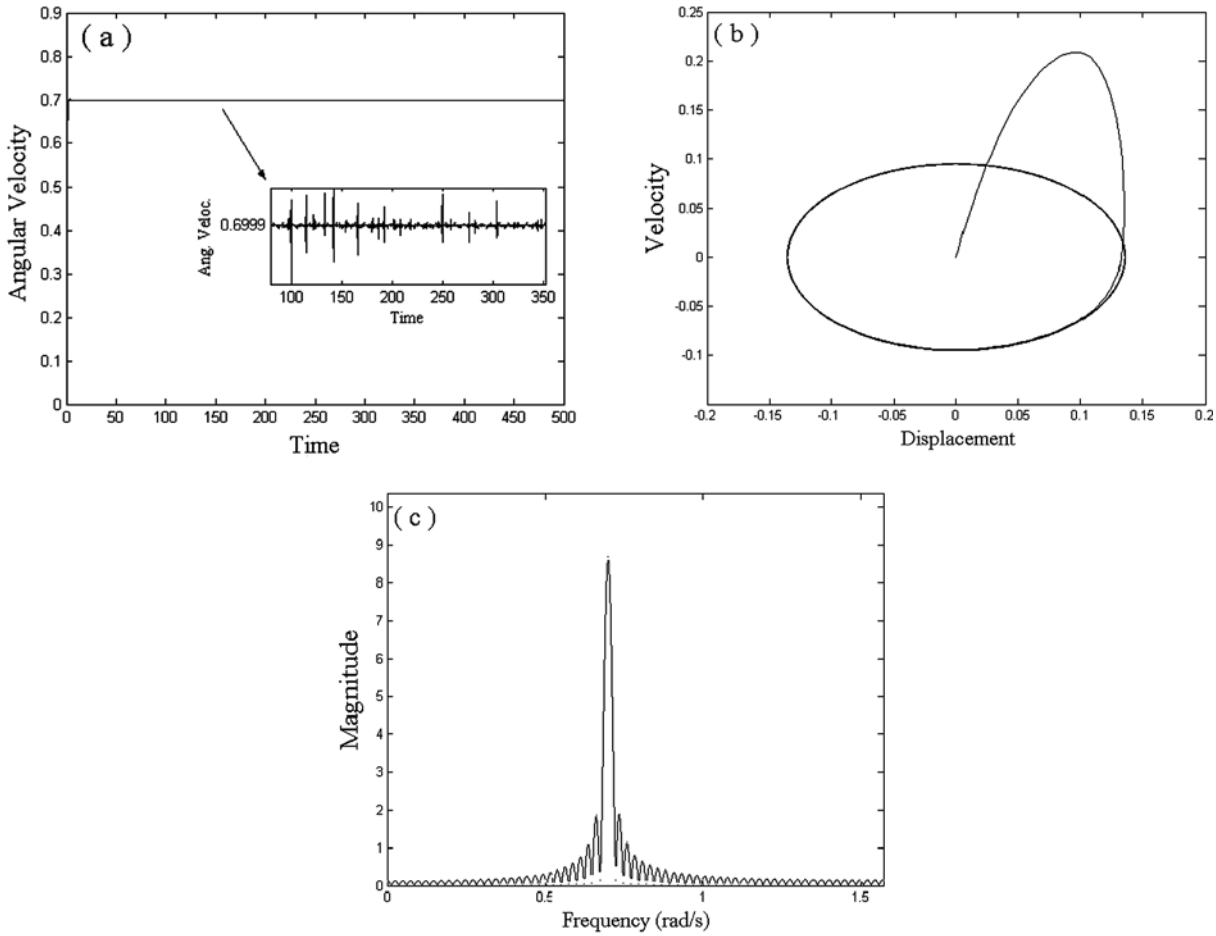

Fig. 3 Controlled system: (**a**) Angular velocity time response, (**b**) Phase portrait, and (**c**) Power spectrum for the $\theta = 0.7$, $\mu = 0.01$, and $\xi_1 = 0.7$

The behavior of the controlled nonideal system is presented in Fig. 3 for $\theta = 0.7$, $\mu = 0.01$, and $\xi_1 = 0.7$.

It can be observed from these figures that feedback control (14) was efficient, reducing the displacements and moving the system to equilibrium point in a lower time then without control.

Now, we use the Poincare section to characterize the dynamic of the system. When there is no control acting on the system, a representative Poincare section shows in Fig. 4(a) a strange attractor behavior of the chaotic motion, but when the control is activated, the chaotic attractor is replaced by one periodic attractor, represented in Fig. 4(b).

4.2 Austenitic phase

In this section, a linear model based controller is designed to stabilize globally and asymptotically the nonideal pseudoelastic system. In this case, the response of the system is considered at higher temperatures ($\theta = 2$), when the alloy is fully austenitic.

The parameters are selected as $\theta = 2$, $\mu = 0.01$, and $\xi_1 = 1.5$, thus we obtained that the system (4) without control possesses a chaotic attractor shown in Fig. 5.

Figure 5 shows an interesting dynamical behavior when we consider $\xi_1 = 1.5$ (resonance regions). We observe that the angular velocity of the rotor is captured in resonance causing instability in the motion of the nonideal SMA system.

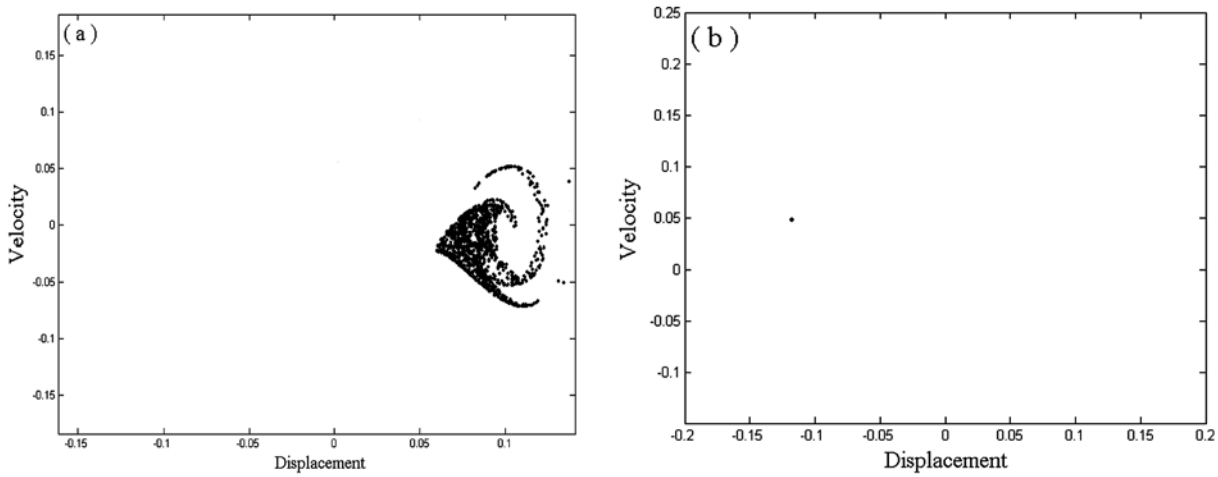

Fig. 4 Poincare section: (**a**) uncontrolled system (strange attractor) and (**b**) controlled system (periodic attractor) for $\theta = 0.7$

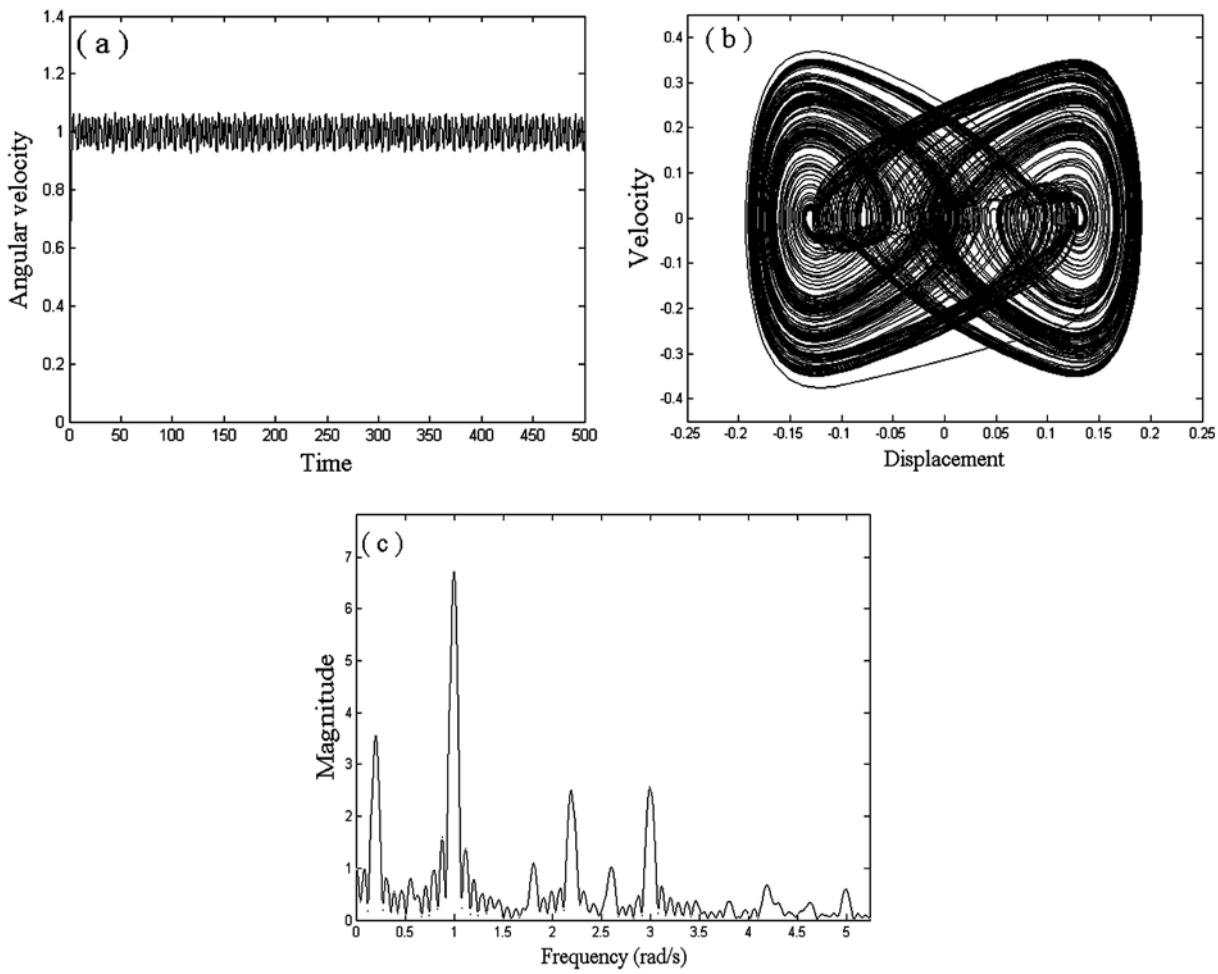

Fig. 5 Uncontrolled system: (**a**) Angular velocity time response, (**b**) Phase portrait, and (**c**) Power spectrum for the $\theta = 2$, $\mu = 0.01$, and $\xi_1 = 1.5$

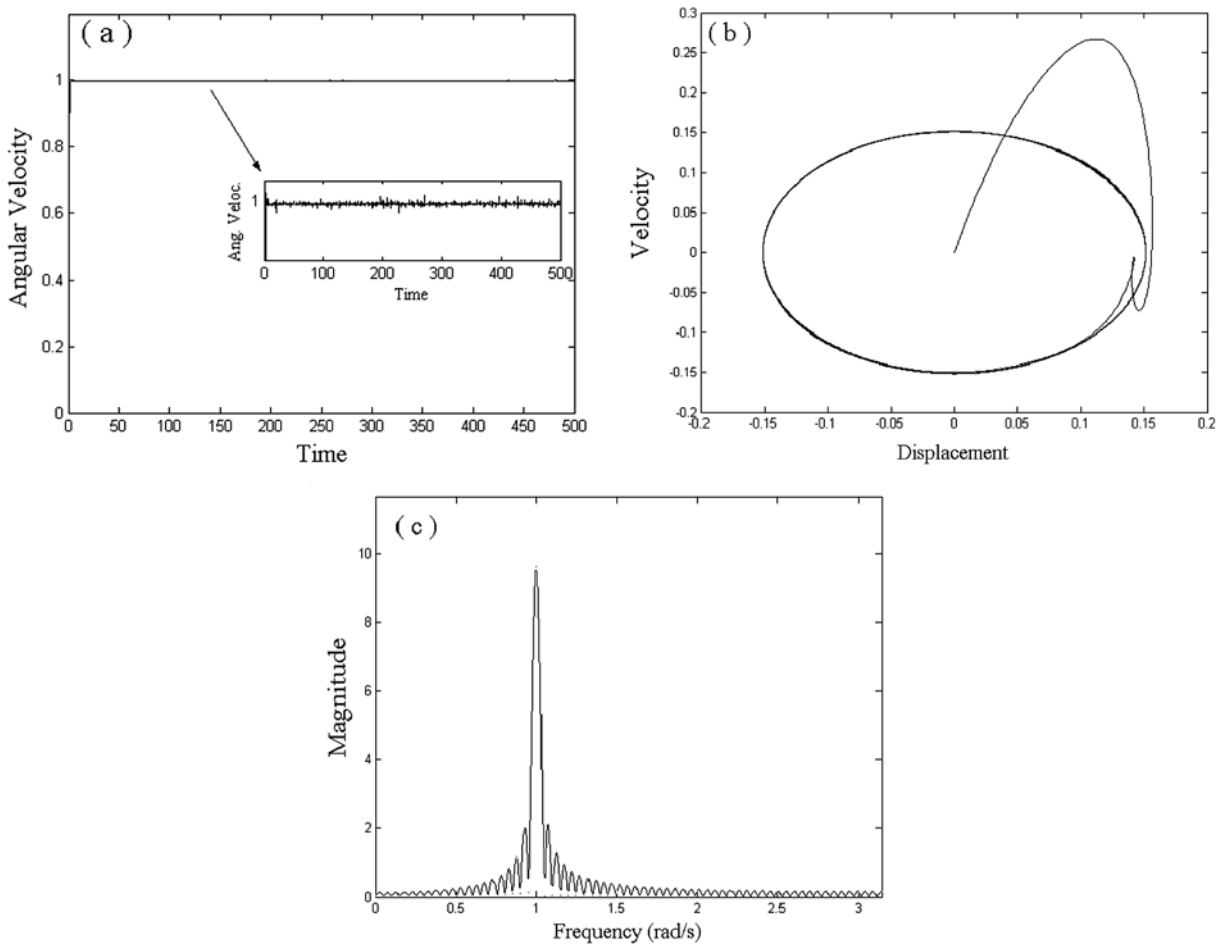

Fig. 6 Controlled system: (**a**) Angular velocity time response, (**b**) Phase portrait, and (**c**) Power spectrum for the $\theta = 2$, $\mu = 0.01$, and $\xi_1 = 1.5$

We analyze the suppression of chaos on the averaging system near the fundamental resonance. Thus, the parameter considered for the desired periodic orbit is $\theta = 2$, $\mu = 0.01$, and $\xi_1 = 1.5$ (value in resonance region). In steady-state phase, (12) has the following form:

$$\tilde{u} = \begin{bmatrix} 0.1515\cos(0.9998t + 17.27) \\ -0.15146\sin(0.9998 + 17.27) \\ 0.9998t \\ 0.9998 \end{bmatrix}. \tag{16}$$

The performance of the linear feedback control of the nonideal system can be seen in Fig. 6. This figure shows the interaction between the nonideal pseudoelastic system and linear controller when the angular velocity of the motor is captured in the resonance region according to control parameter $\xi_1 = 1.5$. Clearly, the control strategy is effective around the resonance frequency, where the angular velocity of the motor is reduced to the average angular velocity.

Here, Poincare section approach is applied again to check the results mentioned above and the excellent agreement has been observed. For $\theta = 2$, $\mu = 0.01$, and $\xi_1 = 1.5$, we plot Poincare section in the Fig. 7.

Again, we use the Poincare section to characterize the dynamic of the system. When there is no control acting on the system, a Poincare section shows in Fig. 7(a) a strange attractor. This behavior is possible because the Poincare section is neither a finite set of points nor a closed orbit, the motion may be chaotic. On the other hand when the control is activated, the chaotic attractor is replaced by one periodic attractor, represented in Fig. 7(b). The solution of the

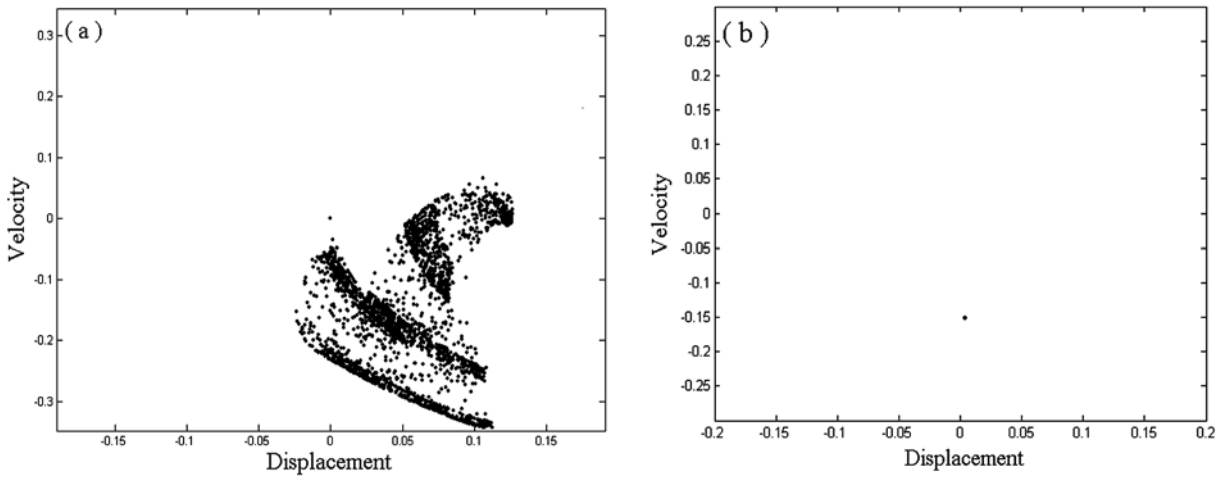

Fig. 7 Poincare section: (**a**) uncontrolled system (strange attractor) and (**b**) controlled system (periodic attractor) for $\theta = 0.7$

controlled system of period-1T in the phase will become one point in the Poincare section.

5 Conclusions

We presented a procedure to suppress chaotic behavior in a nonideal oscillator using the linear feedback control associated with the limited power supply, in such a way that the feedback control alters the angular velocity of the motor. This method is based on the fact that altering the original angular velocity of the DC motor to the averaging angular velocity, one can steer the system trajectory from a chaotic attractor to a periodic orbit, given an improved system performance.

We also remarked that this technique is analytical and it works without dropping any important contribution, which was in the modeling of governing equation of motion.

The method of averaging is used to determine an approximate solution to this controlled nonideal system.

The simulation model for proposed controllers can be implemented through MATLAB™–Simulink®. The numerical results showed the effectiveness of the used linear feedback control. This is a first use of this kind of control on nonideal vibrating system. In Part I [23], we dealt with the ideal problem.

Acknowledgements The authors thank the support of the Brazilian funding Agencies CAPES, FAPESP, and CNPq.

References

1. Han, Y.-L., Xing, D.-J., Xiao, E.-T., Li, A.-Q.: NiTi-wire shape memory alloy dampers to simultaneously damp tension, compression, and torsion. J. Vib. Control **11**(8), 1067–1084 (2005)
2. Williams, K., Chiu, G., Bernhard, R.: Adaptive-passive absorbers using shape memory alloys. J. Sound Vib. **249**(5), 835–848 (2002)
3. Saadat, S., Salichs, J., Noori, M., Hou, Z., Davoodi, H., Bar-On, I., Suzuki, Y., Masuda, A.: An overview of vibration and seismic applications of NiTi shape memory alloy. Smart Mater. Struc. **11**(2), 218–229 (2002)
4. Oberaigner, E.R., Fischer, F.D., Tanaka, K.: On the optimal damping of a vibrating shape memory alloy rod. J. Eng. Mater. Technol. **124**, 97–102 (2002)
5. Dolce, M., Cardone, D., Marnetto, R.: Implementation and testing of passive control devices based on shape memory alloys. Earthquake Eng. Struct. Dyn. **29**, 945–968 (2000)
6. Rogers, C.A.: Active vibration and structural acoustic control of shape memory alloy hybrid composites: experimental results. J. Acoust. Soc. Am. **88**, 2803–2811 (1990)
7. Rogers, C.A., Liang, C., Fuller, C.R.: Modeling of shape memory alloy hybrid composites for structural acoustic control. J. Acoust. Soc. Am. **89**, 210–220 (1991)
8. Nayfeh, A.H., Mook, D.T.: Nonlinear Oscillations. Wiley, New York (1979)
9. Balthazar, J.M., Mook, D.T., Weber, H.I., Brasil, R.M.F.L.R.F., Fenili, A., Belato, D., Felix, J.L.P.: An overview on non-ideal vibrations. Meccanica **38**, 613–621 (2003)
10. Dantas, M.J.H., Balthazar, J.M.: On the existence and stability of periodic orbits in non-ideal problems: general results. J. Appl. Math. Mech. 940–956 (2007)
11. Felix, J.L.P., Balthazar, J.M., Brasil, R.M.F.L.R.F.: On saturation control of a non-ideal vibrating portal frame foundation type shear-building. J. Vib. Control **11**, 121–136 (2005)

12. Balthazar, J.M., Cheshankov, B.I., Ruschev, D.T., Barbanti, L., Weber, H.I.: Remarks on the passage through resonance of a vibrating system with two degrees of freedom, excited by a non-ideal energy source. J. Sound Vib. **239**, 1075–1085 (2001)
13. Souza, S.L.T., Caldas, I.L., Viana, R.L., Balthazar, J.M., Brasil, R.M.L.R.F.: A simple feedback control for a chaotic oscillator with limited power supply. J. Sound Vib. **299**, 664–671 (2007)
14. Souza, S.L.T., Caldas, I.L., Viana, R.L., Balthazar, J.M., Brasil, R.M.L.R.F.: Impact dampers for controlling chaos in systems with limited power supply. J. Sound Vib. **279**, 955–967 (2005)
15. Rafikov, M., Balthazar, J.M.: On a optimal control design for Rössler system. Phys. Lett. A **333**, 241–245 (2004)
16. Rafikov, M., Balthazar, J.M.: On control and synchronization in chaotic and hyperchaotic system via linear control feedback. Commun. Nonlinear Sci. Numer. Simul. **13**, 1246–1255 (2008)
17. Rafikov, M., Balthazar, J.M.: Mathematical modeling and control of population systems: applications in biological pest control. Appl. Math. Comput. **200**, 557–573 (2008)
18. Chavarette, F.R., Balthazar, J.M., Rafikov, M., Hermini, H.A.: On non-linear dynamics and an optimal control synthesis of the action potential of membranes (ideal and non-ideal cases) of the Hodgkin–Huxley (HH) mathematical model. Chaos Solitons Fractals (2008, in press)
19. Savi, M.A., Braga, A.M.B.: Chaotic vibrations of an oscillator with shape memory. J. Braz. Soc. Mech. Sci. Eng. **XV**(1), 1–20 (1993)
20. Felix, J.L.P., Balthazar, J.M., Dantas, M.J.H.: On energy pumping, synchronization and beat phenomenon in a non-ideal structure coupled to an essentially nonlinear oscillator. Nonlinear Dyn. (2008, in press)
21. Piccirillo, V., Balthazar, J.M., Pontes, B.R., Jr., Palacios, J.L.: On a nonlinear and chaotic non-ideal vibrating system, with shape memory alloy (SMA). J. Theor. Appl. Mech. (2008, in press)
22. Zukovic, M., Cveticanin, L.: Chaotic responses in a stable Duffing system on non-ideal type. J. Vib. Control **13**(6), 751–767 (2007)
23. Piccirillo, V., Balthazar, J.M., Pontes, B.R., Jr., Palacios, J.L.: Chaos control of a nonlinear oscillator with shape memory alloy using an optimal linear control: Part I: ideal energy source. Nonlinear Dyn. (2008, in press)